Journal of Solid State Chemistry 184 (2011) 899–904

Contents lists available at ScienceDirect

Journal of Solid State Chemistry

journal homepage: www.elsevier.com/locate/jssc

Synthesis, crystal structures and luminescent properties of two 4*d*–4*f* *Ln*–Ag heterometallic coordination polymers based on anion template

Le-Qing Fan*, Yuan Chen, Ji-Huai Wu*, Yun-Fang Huang

Institute of Materials Physical Chemistry, and the Key Laboratory for Functional Materials of Fujian Higher Education, Huaqiao University, Quanzhou, Fujian 362021, PR China

ARTICLE INFO

Article history:
Received 9 December 2010
Received in revised form
17 February 2011
Accepted 20 February 2011
Available online 26 February 2011

Keywords:
Ln–Ag heterometallic coordination polymer
Crystal structure
Perchlorate anion template
Luminescent properties

ABSTRACT

Two new 4*d*–4*f* *Ln*–Ag heterometallic coordination polymers, $\{[Ln_3Ag_5(IN)_{10}(H_2O)_7]\cdot 4(ClO_4)\cdot 4(H_2O)\}_n$ (*Ln*=Eu (**1**) and Sm (**2**), HIN=isonicotinic acid), have been synthesized under hydrothermal conditions by reactions of Ln_2O_3, $AgNO_3$, HIN and $HClO_4$, and characterized by elemental analysis, IR, thermal analysis and single-crystal X-ray diffraction. It is proved that $HClO_4$ not only adjusts the pH value of the reaction mixture, but also acts as anion template. The structure determination reveals that **1** and **2** are isostructural and feature a novel two-dimensional (2D) layered hetrometallic structure constructed from one-dimensional *Ln*–carboxylate chains and pillared $Ag(IN)_2$ units. The 2D layers are further interlinked through Ag···Ag and Ag···O(ClO_4^-) multiple weak interactions, which form a rare Ag–ClO_4 ribbon in lanthanide–transition metal coordination polymers, to give rise to a three-dimensional supramolecular architecture. Moreover, the luminescent properties of these two compounds have also been investigated at room temperature.

1. Introduction

In recent years, investigations on the design and synthesis of heterometallic lanthanide (*Ln*)–transition metal (TM) coordination polymers have attracted great interests not only for their fascinating structural topology, but also for their potential applications in magnetism, luminescence materials, molecular adsorption, and bimetallic catalysis [1]. A simple method to realize the synthesis of heterometallic *Ln*–TM coordination polymers is by choosing suitable organic ligands acting as linkers between *Ln* and TM ions. But the construction of *Ln*–TM coordination polymers with useful physico-chemical properties and intriguing structural topologies using this method is still a challenging task; the main reason is that there are competitive reactions between *Ln* and TM coordinated to organic ligands [2]. It is fortunate that, according to the hard–soft acid base theory, *Ln* and TM ions have different affinities for O and N donors. Generally, TM ions easily bond to the ligand containing N-donor atoms [3]. However, compared with TM ions, *Ln* ions have high oxo-affinity, high coordination number and low stereochemical preference, which are critical for the construction of different dimensional lanthanide coordination polymers [4]. If a ligand simultaneously contains O- and N-donor atoms, it should be employed to bond to both *Ln* and TM ions to form heterometallic coordination polymers. To date, various ligands, like pyridinecarboxylate [5], pyridylphosphonate [6], imidazolecarboxylate [7], amino acid [8], etc., containing O- and N-donor atoms are used to construct heterometallic *Ln*–TM coordination polymers with interesting structures and properties. Because isonicotinic acid (HIN) is a linear and potentially bridging ligand with O- and N-donor atoms on opposite sides of the molecule as well as the versatile coordination modes [9], we chose HIN to synthesize multidimensional heterometallic *Ln*–TM coordination polymer. On the other hand, the pH value of the reaction mixture has great influence on the structures of *Ln*–TM coordination polymers. So, some inorganic acids, for example HNO_3 or $HClO_4$, are introduced to adjust the pH value of reaction mixture [8a,8b,9b,10]. In 3*d*–4*f* system, it is also found that ClO_4^- acts as anion template [8b,9b]. However, compared to 3*d*–4*f* system, there are relatively little examples that $HClO_4$ or ClO_4^- anion was used to control the synthesis of 4*d*–4*f* compounds [10b,10d]. Therefore, it is worth exploring the potentially templating role of ClO_4^- anion in 4*d*–4*f* system.

In this paper, we report the synthesis, crystal structures and luminescent properties of two new two-dimensional (2D) 4*d*–4*f* *Ln*–Ag heterometallic coordination polymers, $\{[Ln_3Ag_5(IN)_{10}(H_2O)_7]\cdot 4(ClO_4)\cdot 4(H_2O)\}_n$ (*Ln*=Eu (**1**) and Sm (**2**), HIN=isonicotinic acid), prepared under hydrothermal conditions templated by the perchlorate anions and through IN^- as linkers between Ln^{3+} and Ag^+ ions.

2. Experimental section

2.1. Materials and methods

All of the reagent-grade reactants were commercially available and employed without further purification. The powder X-ray

* Corresponding authors. Fax: +86 59522693999.
E-mail addresses: lqfan@hqu.edu.cn (L.-Q. Fan), jhwu@hqu.edu.cn (J.-H. Wu).

0022-4596/$ - see front matter © 2011 Elsevier Inc. All rights reserved.
doi:10.1016/j.jssc.2011.02.019

diffraction (PXRD) data were measured on a DMAX2500 diffractometer. The solid infrared (IR) spectra were obtained from a Nicolet Nexus 470 FT-IR spectrometer between 400 and 4000 cm^{-1} using KBr pellets. Element analyses of carbon, hydrogen and nitrogen were performed with a Vario EL III element analyzer. Thermogravimetric analyses (TGA) were performed on a Netzsch Sta449C thermoanalyzer under N_2 atmosphere in the range of 30–600 °C at a heating rate of 10 °C/min. Fluorescence spectra were obtained at room temperature with the aid of an Edinburgh FLS920 fluorescence spectrophotometer with the polycrystalline sample held between two pieces of fused silica slices. The crystal structures were determined by a Rigaku Mercury CCD area-detector diffractometer and SHELXL crystallographic software of molecular structure.

2.2. Synthesis of $\{[Ln_3Ag_5(IN)_{10}(H_2O)_7]\cdot 4(ClO_4)\cdot 4(H_2O)\}_n$ (Ln=Eu (**1**) and Sm (**2**))

Compound **1** was hydrothermally synthesized under autogenous pressure. A mixture of Eu_2O_3 (0.176 g, 0.5 mmol), $AgNO_3$ (0.170 g, 1 mmol), HIN (0.246 g, 2 mmol) and H_2O (10 mL) was stirred at room temperature until a homogeneous mixture was obtained, and was adjusted to pH=2 by the addition of $HClO_4$ (0.035 g, 0.35 mmol). The mixture was transferred into a Teflon-line autoclave (23 mL) and heated at 170 °C for 7 days and then cooled at rate of 10 °C h^{-1} to room temperature. Yellow prismatic crystals of **1** were recovered by filtration, washed with distilled water, and dried in air (36% yield based on Eu). Anal. Calcd. for **1** (dried) (%): C, 25.63; H, 2.22; N, 4.98. Found: C, 25.89; H, 2.09; N, 4.83. Selected IR data (KBr pellet, cm^{-1}): 3413, 1596, 1542, 1405, 1113, 684.

Compound **2** was prepared with the similar procedure of **1** except that Eu_2O_3 was replaced by Sm_2O_3 (0.174 g, 0.5 mmol). Yellow prismatic crystals of **2** were obtained with the yield of 32% based on Sm. Anal. Calcd. for **2** (dried) (%): C, 25.67; H, 2.22; N, 4.99. Found: C, 25.91; H, 2.11; N, 4.82. Selected IR data (KBr pellet, cm^{-1}): 3420, 1596, 1542, 1412, 1115, 683.

2.3. Determination of crystal structure

The crystallographic data for **1** and **2** were collected on a Rigaku Mercury CCD area-detector equipped with a graphite-monochromated Mo$K\alpha$ radiation (λ=0.71073 Å) at 293(2) K using an ω–2θ scan mode. Absorption corrections were performed by the CrystalClear program [11]. Both structures were solved by direct methods using SHELXS-97 program and refined by full-matrix least-squares refinement on F^2 with the aid of SHELXL-97 program [12]. All non-hydrogen atoms were refined anisotropically. Hydrogen atoms attached to carbon were placed in geometrically idealized positions and refined using a riding model. Hydrogen atoms on water molecules were located from difference Fourier maps and were also refined using a riding model. Crystallographic data (excluding structure factors) for the structure reported in this paper have been deposited with the Cambridge Crystallographic Data Centre as supplementary publication nos. CCDC 802414 for **1** and 802415 for **2**. Copies of the data can be obtained free of charge on application to CCDC, 12 Union Road, Cambridge CB2 1EZ, UK (fax: +44 1223 336-033; e-mail: deposit@ccdc.cam.ac.uk). Some refinement details and crystal data of **1** and **2** are summarized in Table 1. Selected bond lengths of **1** and **2** are shown in Table 2. Selected bond angles of **1** and **2** are gathered in Table S1 in the Supplementary Materials.

Table 1
Crystallographic data and structure refinement parameters for **1** and **2**.

	1	**2**
Empirical formula	$C_{60}H_{62}Ag_5Cl_4Eu_3N_{10}O_{47}$	$C_{60}H_{62}Ag_5Cl_4Sm_3N_{10}O_{47}$
Formula weight	2812.23	2807.40
Crystal system	Monoclinic	Monoclinic
Space group	*Cc*	*Cc*
a (Å)	21.922(12)	21.888(5)
b (Å)	33.730(8)	33.7268(19)
c (Å)	14.948(9)	14.938(3)
β (deg)	130.512(3)	130.540(3)
V (Å^3)	8403(7)	8380(3)
Z	4	4
T (K)	293(2)	293(2)
$D_{calc.}$ (g cm^{-3})	2.223	2.225
μ (mm^{-1})	3.578	3.444
F(0 0 0)	5440	5428
λ (Å)	0.71073	0.71073
Data collected	32,463	32,501
Independent data	17,102	17,158
R_{int}	0.0263	0.0263
θ range (deg)	2.19–27.48	2.16–27.49
Goodness-of-fit on F^2	1.002	1.078
Data/restraints/parameters	1163/24/15581	1162/24/15251
R_1 [$I>2\sigma(I)$][a]	0.0386	0.0376
wR_2 [$I>2\sigma(I)$][b]	0.0996	0.0872
$\Delta\rho$ (maximum/minimum) (e Å^{-3})	2.546/–1.081	1.707/–1.617

[a] $R_1=\sum||F_0|-|F_c||/\sum|F_0|$.
[b] $wR_2=[\sum w(|F_0^2|-|F_c^2|)^2/\sum w(F_0^2)^2]^{1/2}$.

3. Results and discussion

3.1. Synthesis

The compounds **1** and **2** were synthesized from the reaction mixture of Ln_2O_3, $AgNO_3$, HIN, and $HClO_4$ with the mole ratio of 1:2:4:0.7 in water at 170 °C by the hydrothermal technique. However, isomorphous complexes with other Ln^{3+} having larger or smaller ion radii are not obtained. In this system, $HClO_4$ was added to adjust the pH value of the reaction mixture. And it was found that crystals suitable for X-ray single-crystal analysis were obtained only with this ratio. On the other hand, because the ClO_4^- anions locate in the void of the framework of **1** and **2**, and weakly contact with the framework by multiple Ag···O(ClO_4^-) interactions, the ClO_4^- anions can be seen as anion template in this reaction system. And series of experiments have validated the ClO_4^- templating role. Firstly, experiments using HNO_3 in place of $HClO_4$ to adjust pH=2 and as template (NO_3^- with same charge as ClO_4^-) have been carried out to prepare compounds similarly structural to these two compounds, but unfortunately, we were unsuccessful. Secondly, using HNO_3 to adjust pH=2, experiments using $AgClO_4$ instead of $AgNO_3$ give birth to **1** and **2**; however, experiments based on BF_4^- and PF_6^- anions as templates produce no crystal. Thirdly, attempts using other anion templates with different charges such as SO_4^{2-} and PO_4^{3-} proved fruitless. It is supposed that since the size and charge of anions were changed, the length, coordination modes and charges of organic bridging ligands should also be adjusted so as to realize above ideas. This synthetic research is still in progress.

3.2. Structure description

Single-crystal X-ray diffraction analyses reveal that **1** and **2** crystallize in the monoclinic space group *Cc* (Flack parameters of 0.165(9) and 0.006(8) for **1** and **2**, respectively) and possess novel 2D coordination framework constructed by one-dimensional (1D)

Ln–carboxylate chains and pillared $Ag(IN)_2$ units. Because **1** and **2** are isostructural, only the structure of **1** is described in detail. An ORTEP view of **1** is shown in Fig. 1. The asymmetric unit of **1** contains three Eu^{3+} ions, five Ag^+ ions, ten IN^- ligands, seven coordinated water molecules, four uncoordinated water molecules, and four ClO_4^- anions. The Eu(1), Eu(2), and Eu(3) centers all are eight-coordinated and display square antiprismatic coordination environment: five oxygen atoms from five IN^- ligands, three oxygen atoms from three coordinated water molecules for the Eu(1) center; six oxygen atoms from six IN^- ligands, two oxygen atoms from two coordinated water molecules for the Eu(2) and Eu(3) centers. The Eu–O bond lengths vary from 2.310(5) to 2.522(8) Å, and the O–Eu–O bond angles are in the range of 68.8(2)–147.9(2)°, thus being in the normal range observed in other compounds [13]. All five Ag^+ ions exhibit a linear or rare bow-like conformation [10a], being coordinated by two pyridyl nitrogen atoms from two different IN^- ligands with the Ag–N bond lengths being from 2.119(7) to 2.195(7) Å and the N–Ag–N bond angles ranging from 169.1(3)° to 173.3(3)°, all within the range of those observed for other *Ln*–Ag compounds [10]. In this structure, the IN^- ligands have three evidently different coordination modes: one behaves as a bridging ligand to coordinate two Eu^{3+} ions and one Ag^+ ion (Scheme 1a), another also behaves as a bridging ligand, but it coordinates one Eu^{3+} ion and one Ag^+ ion (Scheme 1b), and the third behaving as a terminal ligand only coordinates to one Ag^+ ion (Scheme 1c).

Table 2
Selected bond lengths (Å) for **1** and **2**.

1			
Eu(1)–O(1)	2.374(5)	Eu(3)–O(7)	2.405(5)
Eu(1)–O(8)#1	2.327(5)	Eu(3)–O(14)	2.367(5)
Eu(1)–O(9)	2.393(6)	Eu(3)–O(16)	2.457(6)
Eu(1)–O(11)	2.346(6)	Eu(3)–O(17)	2.327(5)
Eu(1)–O(18)#1	2.370(5)	Eu(3)–O(26)	2.486(8)
Eu(1)–O(21)	2.496(7)	Eu(3)–O(27)	2.493(7)
Eu(1)–O(22)	2.458(7)	Ag(1)–N(1)	2.141(6)
Eu(1)–O(23)	2.499(7)	Ag(1)–N(3)#2	2.147(6)
Eu(2)–O(2)	2.380(6)	Ag(2)–N(2)	2.125(6)
Eu(2)–O(3)	2.375(7)	Ag(2)–N(4)#2	2.123(6)
Eu(2)–O(5)	2.402(6)	Ag(3)–N(6)	2.129(7)
Eu(2)–O(12)	2.310(5)	Ag(3)–N(9)#5	2.119(7)
Eu(2)–O(13)	2.439(6)	Ag(4)–N(5)#6	2.152(6)
Eu(2)–O(15)	2.364(6)	Ag(4)–N(7)	2.160(6)
Eu(2)–O(24)	2.430(8)	Ag(5)–N(8)	2.195(7)
Eu(2)–O(25)	2.522(8)	Ag(5)–N(10)	2.170(7)
Eu(3)–O(4)	2.390(5)	Ag(1)···Ag(4)#3	3.129(2)
Eu(3)–O(6)	2.401(5)	Ag(2)···Ag(5)#4	3.239(2)
2			
Sm(1)–O(1)	2.389(5)	Sm(3)–O(7)	2.414(5)
Sm(1)–O(8)#1	2.338(5)	Sm(3)–O(14)	2.379(5)
Sm(1)–O(9)	2.402(5)	Sm(3)–O(16)	2.454(5)
Sm(1)–O(11)	2.352(6)	Sm(3)–O(17)	2.330(5)
Sm(1)–O(18)#1	2.385(5)	Sm(3)–O(26)	2.500(7)
Sm(1)–O(21)	2.507(6)	Sm(3)–O(27)	2.500(6)
Sm(1)–O(22)	2.453(6)	Ag(1)–N(1)	2.142(6)
Sm(1)–O(23)	2.513(6)	Ag(1)–N(3)#2	2.151(6)
Sm(2)–O(2)	2.394(5)	Ag(2)–N(2)	2.129(6)
Sm(2)–O(3)	2.397(6)	Ag(2)–N(4)#2	2.119(6)
Sm(2)–O(5)	2.406(5)	Ag(3)–N(6)#5	2.133(6)
Sm(2)–O(12)	2.340(5)	Ag(3)–N(9)	2.123(6)
Sm(2)–O(13)	2.439(5)	Ag(4)–N(5)#5	2.152(6)
Sm(2)–O(15)	2.359(5)	Ag(4)–N(7)	2.158(6)
Sm(2)–O(24)	2.433(8)	Ag(5)–N(8)	2.185(7)
Sm(2) –O(25)	2.521(8)	Ag(5)–N(10)	2.172(7)
Sm(3)–O(4)	2.403(6)	Ag(1)···Ag(4)#3	3.1248(13)
Sm(3)–O(6)	2.393(5)	Ag(2)···Ag(5)#4	3.2441(14)

Symmetry codes for **1**: #1 *x*, *y*, 1+*z*; #2 *x*, −*y*, 1/2+*z*; #3 −1/2+*x*, −1/2+*y*, *z*; #4 1/2+*x*, 1/2−*y*; 1/2+*z*; #5 *x*, 1−*y*, 1/2+*z*; #6 *x*, 1−*y*, −1/2+*z*. Symmetry codes for **2**: #1 *x*, *y*, −1+*z*; #2 *x*, −*y*, −1/2+*z*; #3 +1/2+*x*, −1/2+*y*, *z*; #4 −1/2+*x*, 1/2−*y*; −1/2+*z*; #5 *x*, 1−*y*, 1/2+*z*.

Scheme 1a–c, respectively). However, the 4–2–2–4 type is very rare. The 1D Eu–carboxylate chains are connected by $Ag(IN)_2$ pillars to form 2D Eu–IN–Ag layer extending *bc* plane (Fig. 2), in which the $Ag(IN)_2$ pillars are not parallel to each other.

The Eu^{3+} ions are alternately bridged by two, three or four μ-carboxylate group of IN^- ligands in a 4–2–2–4 (the number indicates the number of the bridges) mode to construct a 1D Eu–carboxylate chain along *c*-axis with the Eu···Eu distances of 5.333(4), 5.260(3) and 4.593(3) Å, respectively (Fig. 2 and Scheme 2d). It is worthy that, up to date, the types of the chains formed by Ln^{3+} ions and IN^- ligands that have been documented are mainly 1–1–1–1 [9c], 2–1–2–1 [10b], and 2–2–2–2 [14] types (Scheme 2a–c, respectively). However, the 4–2–2–4 type is very rare. The 1D Eu–carboxylate chains are connected by $Ag(IN)_2$ pillars to form 2D Eu–IN–Ag layer extending *bc* plane (Fig. 2), in which the $Ag(IN)_2$ pillars are not parallel to each other.

It should be noted that, in this structure, there are some weak interactions (Fig. 3). The Ag(1)···Ag(4) and Ag(2)···Ag(5) distances are 3.1248(13) and 3.2441(14) Å, respectively, which are slightly smaller than the sum of the van der Waals radii for two silver atoms (3.44 Å) [10b], thus indicating Ag···Ag weak interactions. Meanwhile, all five Ag^+ ions weakly contact with neighboring oxygen atoms of ClO_4^- anions ($Cl(2)O_4^-$, $Cl(3)O_4^-$ and $Cl(4)O_4^-$) with the Ag···O distances being from 2.688 (16) to 3.195(19) Å, which are also less than the sum of the van der Waals radii of Ag and O atoms (3.20 Å) [10b], indicating the weak interactions between Ag and ClO_4^- anions. As shown in Fig. 3, the Ag···Ag and Ag···O(ClO_4^-) multiple weak interactions result in the

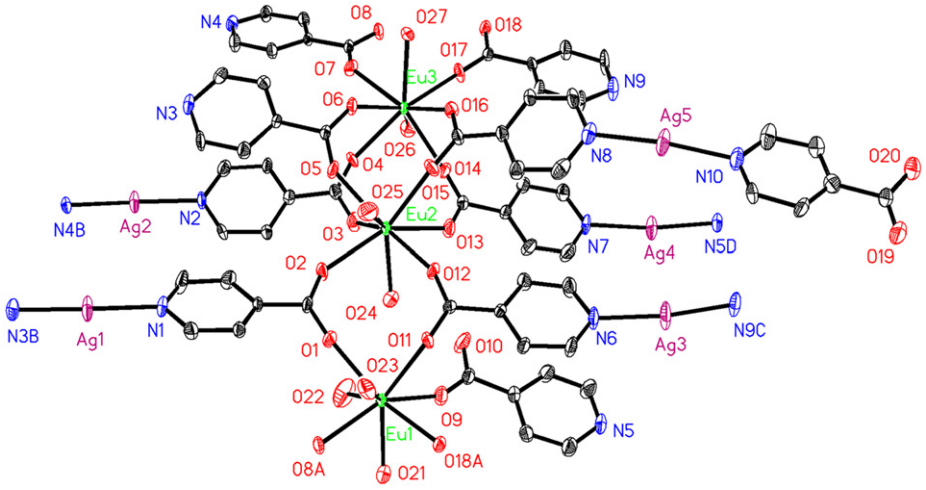

Fig. 1. ORTEP plot of the asymmetric unit of **1** (30% probability ellipsoids). All H atoms, ClO_4^- anions and uncoordinated water molecules are omitted for clarity. Symmetry codes: A *x*, *y*, 1+*z*; B *x*, –*y*, 1/2+*z*; C *x*, 1−*y*, 1/2+*z*; and D *x*, 1−*y*, –1/2+*z*.

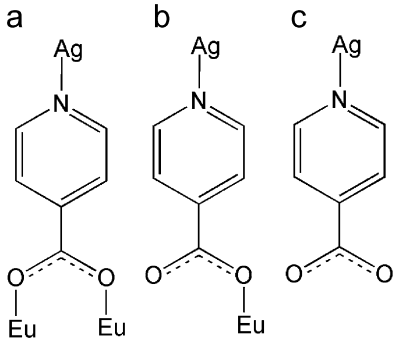

Scheme 1. Coordination modes of the IN^- ligand in **1**.

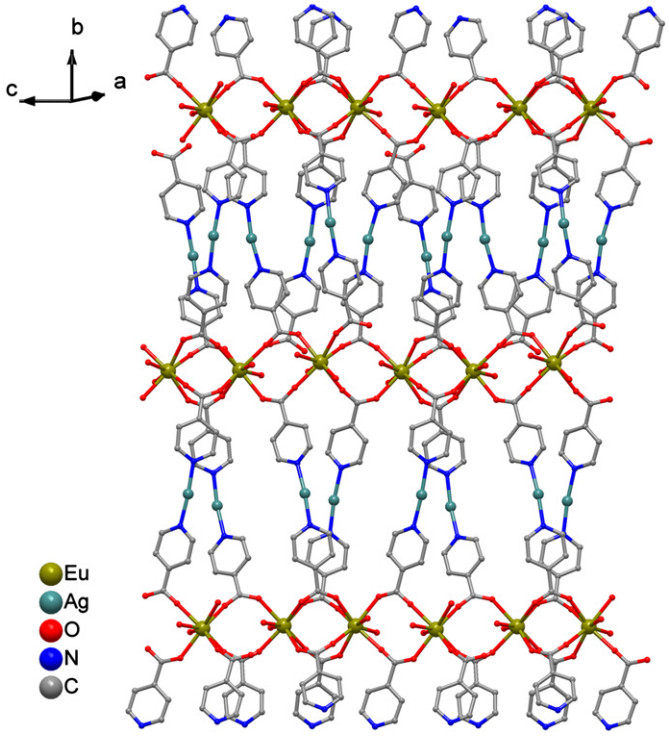

Fig. 2. View of the 2D Eu–IN–Ag layer of **1** extending along *bc* plane.

formation of 1D $Ag_5(ClO_4)_3$ ribbon along *c*-axis. Such a 1D Ag–ClO_4 ribbon in *Ln*–TM system, to the best of our knowledge, never been reported in the literature. The 1D $Ag_5(ClO_4)_3$ ribbons link the 2D Eu–IN–Ag layers to give rise to three-dimensional (3D) supramolecular architecture (Fig. 4). The $Cl(1)O_4^-$ anion and uncoordinated water molecules lie in the voids of this 3D supramolecular architecture by hydrogen bonding interactions, which further stabilize this structure.

3.3. PXRD analysis

The as-synthesized samples of **1** and **2** were characterized by powder X-ray diffraction at room temperature. The PXRD patterns for the bulk product are in fair agreement with the patterns based on single-crystal X-ray solution in position, indicating the phase purity of the as-synthesized samples of **1** and **2** (see Figs. S1 and S2 in the Supplementary Materials). The difference in reflection intensities between the simulated and experimental patterns was due to the variation in preferred orientation of the powder sample during collection of the experimental PXRD data.

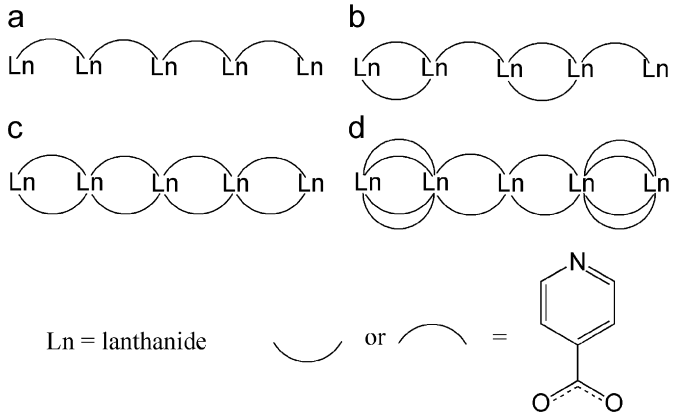

Scheme 2. Important chain-like structural types of IN^- ligands bridging Ln^{3+} ions: (a) 1–1–1–1; (b) 2–1–2–1; (c) 2–2–2–2; and (d) 4–2–2–4 types, in which the number indicates the number of the bridges.

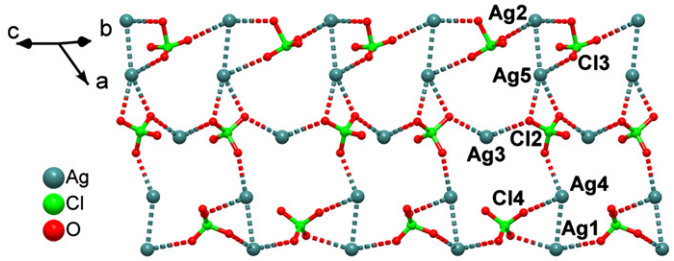

Fig. 3. View of the 1D $Ag_5(ClO_4)_3$ ribbon in **1** constructed by Ag···Ag and Ag···O(ClO_4^-) multiple weak interactions along *c*-axis.

3.4. IR spectroscopy

In the IR spectrum of **1** (see Fig. S3(a) in the Supplementary Materials), the strong and broad absorption band in the range of about 3413 cm^{-1} is assigned as characteristic peak of OH vibration. The strong vibrations appearing at 1596 and 1405 cm^{-1} correspond to the asymmetric and symmetric stretching vibrations of carboxylate group, respectively. The absence of strong bands in the range of 1690–1730 cm^{-1} indicates that all carboxyl groups of HIN are deprotonated. The strong vibration appearing around 1113 cm^{-1} corresponds to the Cl–O stretching vibration [15]. The IR spectrum of **2** exhibits similar feature as that of **1**(see Figs. S5(a) and (b) in the Supplementary Materials).

3.5. Thermal stability

The thermal stability of **1** and **2** was examined by TGA in N_2 atmosphere from 30 to 600 °C (see Figs. S4 and S5 in the Supplementary Materials). They show the similar thermal behavior. The lattice-water and coordinated water molecules were gradually lost in the temperature ranging 30–140 °C (calcd./found: 7.04/6.88% for **1**, 7.05/6.85% for **2**), Above this temperature, the weight loss is due to the decomposition of the IN^- ligands, perchlorate anions and the collapse of the whole framework of these two compounds.

3.6. Luminescent properties

Because of the excellent luminescent properties of Eu^{3+} and Sm^{3+} ions, the luminescent properties of **1** and **2** in solid state were investigated at room temperature. As shown in Fig. 5, the emission spectrum of **1** with an excitation wavelength of 292 nm

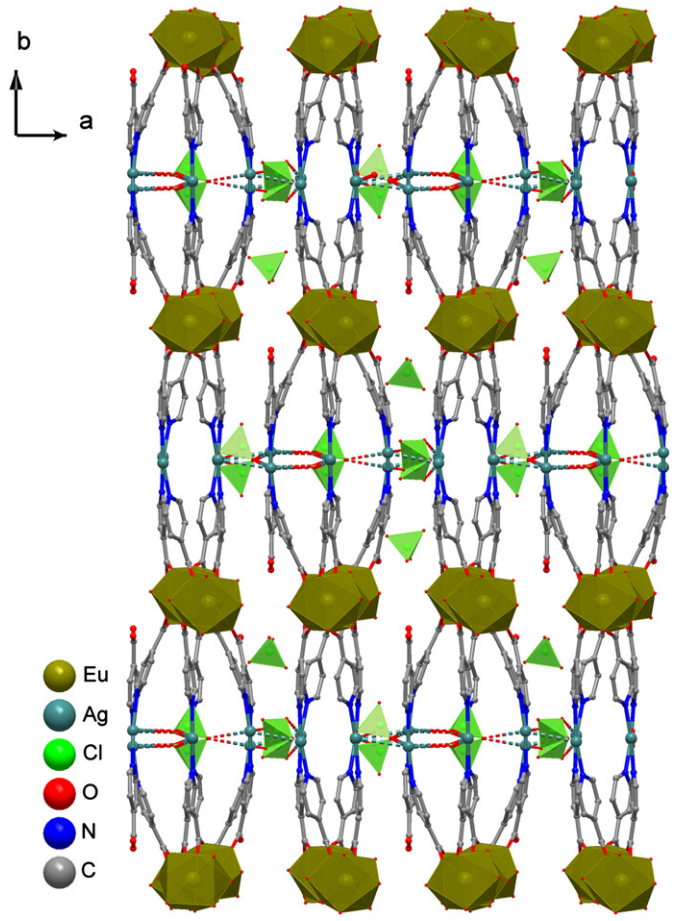

Fig. 4. View of the 3D supramolecular architecture of **1** builded by Ag···Ag and Ag···O(ClO_4^-) multiple weak interactions.

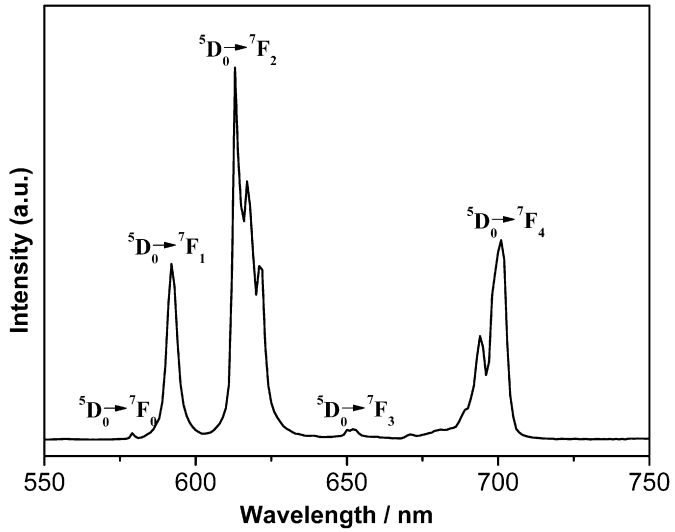

Fig. 5. Solid-state emission spectrum for **1** in the solid state at room temperature (excited at 292 nm).

displays the characteristic transitions of $^5D_0 \rightarrow {}^7F_n$ ($n=0 \rightarrow 4$) of Eu^{3+} ions at 579, 592, 612, 653, and 701 nm, respectively [16]. The appearance of the symmetry-forbidden emission $^5D_0 \rightarrow {}^7F_0$ at 579 nm indicates that Eu^{3+} ions occupy sites with low symmetry and without an inversion center, which is confirmed by X-ray structural structure of **1**. The band at 592 nm can be attributed to

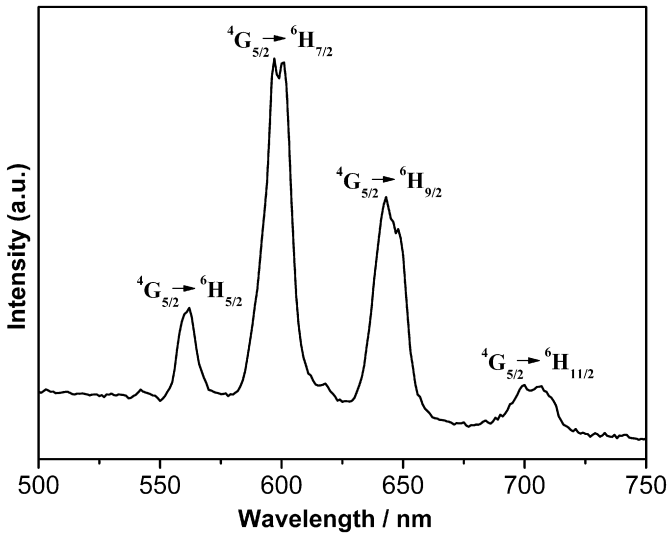

Fig. 6. Solid-state emission spectrum for **2** in the solid state at room temperature (excited at 290 nm).

magnetic-dipolar $^5D_0 \rightarrow {}^7F_1$ transition. And the band at 612 nm can be assigned to electric-dipolar $^5D_0 \rightarrow {}^7F_2$ transition. The intensity of the $^5D_0 \rightarrow {}^7F_2$ transition increases with the decrease of the site symmetry of Eu^{3+} ions. The intensity ratio of $I(^5D_0 \rightarrow {}^7F_2)/I(^5D_0 \rightarrow {}^7F_1)$ is equal to ca. 2.12, which also denotes the noncentrosymmetric coordination geometry of the Eu^{3+} ions in **1**. The most intense transition is $^5D_0 \rightarrow {}^7F_2$, which implies intense red luminescence of **1**. Fig. 6 shows the emission spectrum of **2** upon excitation of 290 nm. It contains four emission peaks at 562, 599, 642, and 698 nm, which are attributed to the characteristic emission of $^4G_{5/2} \rightarrow {}^6H_J$ ($J=5/2$, 7/2, 9/2, and 11/2, respectively) transitions of the Sm^{3+} ions [17]. The high intensity of the $^4G_{5/2} \rightarrow {}^6H_{7/2}$ transition at 599 nm implies the red luminescence of **2**. It can be found that, in **1** and **2**, ligand-to-silver energy transfer is unobvious, which is testified by no other emission peaks existing in the emission spectrum except the characteristic emission peaks of Eu^{3+} and Sm^{3+} ions, respectively.

4. Conclusions

In conclusion, we have successfully hydrothermally synthesized two 4*d*–4*f* *Ln*–Ag heterometallic coordination polymers by the introduction of anion template ClO_4^-. X-ray crystallography revealed that **1** and **2** are isostructural, in which pillared Ag(IN) subunits link the 1D *Ln*–carboxylate chains to produce 2D layers, which are further connected by Ag···Ag and Ag···O(ClO_4^-) multiple weak interactions to form 3D supramolecular architecture. The successful synthesis of these two compounds suggest that novel 4*d*–4*f* hetrometallic polymers with particular functions could be designed and synthesized by the choice of suitable organic O- and N-donor ligands as well as a series of anionic templates with different charges and sizes.

Acknowledgments

This work was supported financially by the National High Technology Research and Development Program of China (863 Program) (no. 2009AA03Z217), the National Natural Science Foundation of China (no. 90922028), the Young Talent Program of Fujian Province (no. 2007F3060) and the Fund of Fujian Provincial Key Laboratory of Nanomaterials (no. NM10-5).

Appendix A. Supplementary data

Selected bond angles, IR spectra, simulated and experimental PXRD patterns, and TG curves for **1** and **2** are provided as supplementary materials.

Supplementary data associated with this article can be found in the online version at doi:10.1016/j.jssc.2011.02.019.

References

[1] (a) J.-W. Cheng, S.-T. Zheng, G.-Y. Yang, Inorg. Chem. 47 (2008) 4930;
(b) V. Mereacre, Y. Lan, R. Clérac, A.M. Ako, I.J. Hewitt, W. Wernsdorfer, G. Buth, C.E. Anson, A.K. Powell, Inorg. Chem. 49 (2010) 5293;
(c) X.-Q. Zhao, Y.-H. Lan, B. Zhao, P. Cheng, C.E. Anson, A.K. Powell, Dalton Trans. 39 (2010) 4911;
(d) Y.-M. Xie, W.-T. Chen, J.-H. Wu, J. Solid State Chem. 181 (2008) 1853.

[2] (a) M. Shibasaki, N. Yoshikawa, Chem. Rev. 102 (2002) 2187;
(b) J. Inanaga, H. Furnuno, T. Hayano, Chem. Rev. 102 (2002) 2211.

[3] (a) J.-P. Zhang, X.-M. Chen, J. Am. Chem. Soc. 131 (2009) 5516;
(b) L.-Q. Fan, J.-H. Wu, Y.-F. Huang, J. Solid State Chem. 180 (2007) 3479;
(c) L.-Q. Fan, J.-H. Wu, Y.-F. Huang, J.-M. Lin, Solid State Sci. 12 (2010) 558.

[4] (a) Y.-P. Cai, G.-B. Li, Q.-G. Zhan, F. Sun, J.-G. Zhang, S. Gao, A.-W. Xu, J. Solid State Chem. 178 (2005) 3729;
(b) Z.-Y. Li, J.-W. Dai, N. Wang, H.-H. Qiu, S.-T. Yue, Y.-L. Liu, Cryst. Growth Des. 10 (2010) 2746;
(c) X.-J. Gu, D.-F. Xue, Cryst. Growth Des. 6 (2006) 2551.

[5] (a) Y.-P. Cai, X.-X. Zhou, Z.-Y. Zhou, S.-Z. Zhu, P.K. Thallapally, J. Liu, Inorg. Chem. 48 (2009) 6341;
(b) X.-M. Lin, Y. Ying, L. Chen, H.-C. Fang, Z.-Y. Zhou, Q.-G. Zhan, Y.-P. Cai, Inorg. Chem. Commun. 12 (2009) 316;
(c) X.-J. Gu, D.-F. Xue, CrystEngComm 9 (2007) 471;
(d) X.-Q. Zhao, B. Zhao, W. Shi, P. Cheng, CrystEngComm 11 (2009) 1261;
(e) B. Zhao, X.-Q. Zhao, Z. Chen, W. Shi, P. Cheng, S.-P. Yan, D.-Z. Liao, CrystEngComm 10 (2008) 1144;
(f) G.-X. Liu, Y.-Y. Xu, X.-M. Ren, S. Nishihara, R.-Y. Huang, Inorg. Chim. Acta 363 (2010) 3727.

[6] Y.-S. Ma, Y. Song, L.-M. Zheng, Inorg. Chim. Acta 361 (2008) 1363.

[7] (a) Y.-G. Sun, X.-M. Yan, F. Ding, E.-J. Gao, W.-Z. Zhang, F. Verpoort, Inorg. Chem. Commun. 11 (2008) 1117;
(b) Q. Zhang, Y.-X. Zheng, C.-X. Liu, Y.-G. Sun, E.-J. Gao, Inorg. Chem. Commun. 12 (2009) 523.

[8] (a) J.-J. Zhang, S.-M. Hu, S.-C. Xiang, T.-L. Sheng, X.-T. Wu, Y.-M. Li, Inorg. Chem. 45 (2006) 7173;
(b) J.-J. Zhang, T.-L. Sheng, S.-Q. Xia, G. Leibeling, F. Meyer, S.-M. Hu, R.-B. Fu, S.-C. Xiang, X.-T. Wu, Inorg. Chem. 43 (2004) 5472.

[9] (a) L.-J. Han, W.-L. Zhou, Y.-H. Yang, Y. Xu, Inorg. Chem. Commun. 12 (2009) 385;
(b) Y.-W. Li, Y.-H. Wang, Y.G. Li, E.-B. Wang, J. Solid State Chem. 181 (2008) 1485;
(c) Y.-K. He, H.-Y. An, Z.-B. Han, Solid State Sci. 11 (2009) 49;
(d) Z.-Y. Li, J.-W. Dai, S.-T. Yue, Y.-L. Liu, CrystEngComm 12 (2010) 2014.

[10] (a) Y.-P. Cai, Q.-Y. Yu, Z.-Y. Zhou, Z.-J. Hu, H.-C. Fang, N. Wang, Q.-G. Zhan, L. Chen, C.-Y. Su, CrystEngComm 11 (2009) 1006;
(b) Y. Cai, Z.-H. Liu, J.-X. Mou, H. Deng, M. Zeller, CrystEngComm 12 (2010) 277;
(c) Y.-K. He, Z.-B. Han, Inorg. Chem. Commun. 10 (2007) 1523;
(d) Y.-C. Qiu, H.-G. Liu, Y. Ling, H. Deng, R.-H. Zeng, G.-Y. Zhou, M. Zeller, Inorg. Chem. Commun. 10 (2007) 1399.

[11] Rigaku, CrystalClear, version 1.3.6, Rigaku/MSC, Tokyo, Japan, 2005.

[12] (a) G.M. Sheldrick, SHELXS-97, program for the solution of crystal structures, University of Göttingen, Germany, 1997;
(b) G.M. Sheldrick, SHELXL-97, program for the refinement of crystal structures, University of Göttingen, Germany, 1997.

[13] X.-D. Zhu, S.-Y. Gao, Y.-F. Li, H.-X. Yang, G.-L. Li, B. Xu, R. Cao, J. Solid State Chem. 182 (2009) 421.

[14] (a) M.C. Mondal, O. Sengupta, P. Dutta, M. Seehra, S.K. Nayak, P.S. Mukherjee, Inorg. Chim. Acta 362 (2009) 1913;
(b) Z.-Y. Li, N. Wang, J.-W. Dai, S.-T. Yue, Y.-L. Liu, CrystEngComm 11 (2009) 2003.

[15] (a) Q.-Y. Lian, C.-D. Huang, R.-H. Zeng, Y.-C. Qiu, J.-X. Mou, H. Deng, M. Zeller, Z. Anorg. Allg. Chem. 635 (2009) 393;
(b) D.-Y. Ma, H.-L. Liu, Y.-W. Li, Inorg. Chem. Commun. 12 (2009) 883.

[16] (a) A. Bettencourt-Dias, S. Vsiwanathan, Chem. Commun. (2004) 1024;
(b) M.-S. Chen, Z. Su, M. Chen, S.-S. Chen, Y.-Z. Li, W.-Y. Sun, CrystEngComm 12 (2010) 3267.

[17] J.-W. Cheng, S.-T. Zheng, G.-Y. Yang, Dalton Trans. (2007) 4059.